Neural mechanisms driving hunger-induced changes in sensory perception and behavior in *Caenorhabditis elegans*

Hiu E. Lau[1,2], Zachary T. Cecere[2,3,4], Zheng Liu[2], Claire J. Yang[2], Tatyana O. Sharpee[3,4], and Sreekanth H. Chalasani[1,2,3]

[1] Division of Biological Sciences, University of California, San Diego, La Jolla, CA 92093, USA.

[2] Molecular Neurobiology Laboratory, The Salk Institute for Biological Studies, La Jolla, CA 92037, USA.

[3] Neurosciences Graduate Program, University of California, San Diego, La Jolla, CA 92093, USA.

[4] Computational Neurobiology Laboratory, The Salk Institute for Biological Studies, La Jolla, CA, 92037, USA.

Author for correspondence: schalasani@salk.edu

Summary

While much is known about how external cues affect neural circuits, less is known about how internal states modify their function. We acutely food-deprived *C. elegans* and analyzed its responses in integrating attractant and repellent signals. We show that food deprivation leads to a reversible decline in repellent sensitivity; with no effect on appetitive behavior allowing animals to engage in higher risk behavior. Multiple tissues including the intestine and body wall muscles use a conserved transcription factor, MondoA, to detect the lack of food and release AEX-5 convertase processed peptides from dense core vesicles. Subsequently, ASI chemosensory neurons use the DAF-2 insulin receptor and non-canonical signaling to integrate the tissue-released peptide signals modifying their stimulus-evoked adaptation rate. We suggest that altering ASI neuronal dynamics affects its function and modifies behavior. Together, these studies show how internal state signals modify sensory perception and risk assessment to generate flexible behaviors.

Introduction

Animals have evolved intricate mechanisms to detect relevant environmental cues as well as integrate information about various internal states including hunger and sleep (Sternson et al., 2013; Taghert and Nitabach, 2012). While progress has been made in decoding the neural circuits processing environmental changes, less is known about the machinery that integrates information about internal states. Of particular importance is nutritional status, which has a profound effect on animal survival and elicits dramatic changes in food-seeking behaviors (Atasoy et al., 2012). Moreover, multiple species have been shown to alter their behavior during periods of starvation (Gillette et al., 2000; Inagaki et al., 2014; Kawai et al., 2000; Sengupta, 2013). This is thought to be achieved by constant crosstalk between the central nervous system and the various peripheral organs (Dietrich and Horvath, 2013).

In mammals, signals from peripheral tissues (hormones and nutrients), most notably the gut-released polypeptide ghrelin, trigger neuronal changes and affect behaviors (Kojima et al., 1999; Tschop et al., 2000). Ghrelin acts on hypothalamic neurons that express agouti-related protein (AGRP) and neuropeptide Y (NPY) (Andrews et al., 2008; Cowley et al., 2003), as well as other brain regions to increase food intake (Carlini et al., 2004; Malik et al., 2008). In contrast, leptin and insulin peptides released from adipose tissue and the pancreas respectively, act to suppress feeding behavior (Air et al., 2002). Apart from feeding behaviors, these peptide signals also influence neural circuits regulating anxiety (Dietrich et al., 2015), indicating that this signaling has a broader role in modulating brain function. Moreover, malfunction of peripheral organ-nervous system communication axis results in a number of metabolic disorders, including diabetes and obesity (Dietrich and Horvath, 2012; Muller et al., 2015). Despite the importance of this physiological process, the precise neuronal machinery integrating metabolic signals and modifying behaviors remains unknown.

The nematode *Caenorhabditis elegans* with just 302 neurons (White et al., 1986), 20 cells in its intestine (McGhee, 2007) and 95 body wall muscle cells (Moerman and Williams, 2006) provides a unique opportunity for a high-resolution analysis of how the nervous system integrates internal signals. Previous studies have shown that *C. elegans*, similar to mammals, exhibits a number of behavioral, physiological and metabolic changes in response to altered nutritional status. When worms are removed from food, they exhibit a 50% reduction in their

feeding rate (Avery, 1993). When returned to food, starved animals temporarily feed faster than well-fed animals (Avery and Horvitz, 1990), suggesting that feeding is not a simple reflex to food stimulus but can be modified by experience. Moreover, upon food deprivation, *C. elegans* hermaphrodites will retain eggs (Trent et al., 1983), are unlikely to mate with males (Lipton et al., 2004) and initiate altered foraging behaviors (Gray et al., 2005; Hills et al., 2004; Sawin et al., 2000). Moreover, many molecules that signal hunger are conserved between *C. elegans* and vertebrates. For example, neuropeptide Y (NPY) signaling influences feeding behaviors in nematodes and mammals (de Bono and Bargmann, 1998; Mercer et al., 2011; Nassel and Wegener, 2011). Similar effects are also seen with insulin and dopamine signaling, which seem to act via modifying chemosensory activity and behavior in nematodes (Chalasani et al., 2010; Ezcurra et al., 2011) and on mammalian hypothalamic and mid-brain circuits respectively (Air et al., 2002; Berthoud, 2011; Figlewicz and Sipols, 2010) to modify feeding behavior.

Here we use *C. elegans* to dissect the machinery integrating internal food signals and modifying behaviors. We combined acute food deprivation with a behavioral assay that quantifies the animal's ability to integrate both toxic and food-related signals, mimicking a simplified real world scenario. In this sensory integration assay, animals cross a toxic copper barrier (repellent) and chemotax towards a point source of a volatile odor, diacetyl (attractant) (Ishihara et al., 2002). We show that food-deprived animals have reduced sensitivity to the repellent and cross the copper barrier more readily than well-fed animals. Moreover, we find that multiple internal tissues sense the lack of food, release peptides and use non-canonical insulin signaling to alter the adaptation rate of chemosensory neurons. This altered neuronal state allows animals to reduce their avoidance to repellents and undertake a higher risk strategy in their search for food.

Results

Acute food deprivation specifically alters repellent-driven behaviors

Animals simultaneously integrate both attractant and repellent signals from their environment to generate appropriate behavioral readouts. To mimic these interactions, animals are exposed to a copper repellent barrier and a gradient of a volatile attractant, diacetyl (Ishihara et al., 2002). The proportion of animals that cross the copper barrier are counted and expressed as an integration

index (Figure 1A). We analyzed the behavior of well-fed wild-type animals and found that few cross the copper barrier and locomote towards the spot of the diacetyl (white bar, Figure 1B, Table S1 and Movie S1). In contrast, when animals are food-deprived for 3 hours, we observe an ~100% increase in the number of animals crossing the copper barrier (dark bar, Figure 1B, Table S1 and Movie S2). Moreover, we found that food-deprived animals cross the repellent barrier throughout the entire 45-minute assay suggesting a broad change in behavior (Figure S1A). Food-deprived animals also do not alter locomotory speed indicating that their general movement is not modified (Figure S1B). Also, this effect is not specific to diacetyl, as food-deprived animals also cross the copper barrier more when paired with other volatile attractants, isoamyl alcohol or benzaldehyde (Figure S1C). The proportion of animals crossing the copper barrier in both well-fed and food-deprived states is a function of both attractant and repellent concentrations (Figures S1D-E and Table S1). Together, our results show that food-deprived animals cross the repellent barrier more readily than well-fed animals.

Next, we tested whether food deprivation affects the sensitivity to repellents or attractants independently. We analyzed the behavior of well-fed and food-deprived animals on assay plates with either copper or odor gradients alone. We found that food-deprived animals crossed the copper barrier more readily than well-fed animals, suggesting that their responsiveness to copper is reduced (Figure 1C, Figure S1F and Table S1). In contrast, food-deprived animals did not alter their attraction to diacetyl or other volatile attractants (Figure 1C and Figure S1G). Given the small number of animals that cross the copper barrier alone (Figure 1B, a high % increase from well-fed value results from low integration index in the well-fed condition, Table S1), we continued to pair copper with the diacetyl attractant for further analysis. We found that food-deprived animals have reduced sensitivity to copper, intermediate concentrations of fructose and salt, but not quinine, 2-nonanone and other concentrations of fructose and salt (Figure S1H). We suggest that copper and these intermediate concentrations of salt and fructose are environmental cues that *C. elegans* might have evolved to detect and reducing sensitivity to these cues enables the animal to use a higher risk food search strategy.

Food deprivation reversibly modifies animal behavior

We probed the time course of the food-deprivation effect on animal behavior. We found that animals need to be food deprived for at least 2 hours before they showed a reduction in their copper sensitivity with a maximum effect at 3 hours (Figure 1D). We also found that animals did not deplete their fat stores during the 3-hour food deprivation (Figure S2A-D), suggesting that this behavior change is likely to be independent of fat metabolism. Next, we asked whether the food-deprivation effect was reversible. We food-deprived animals for 3 hours and then returned them to food for different durations and analyzed animal behavior after the food experience. We found that food-deprived animals that had been returned to food for 5 hours reverted their copper avoidance behavior to well-fed behavior (Figure 1E). These results indicate that food deprivation reversibly reduces copper avoidance.

C. elegans has been shown to evaluate multiple aspects of the food experience, including changes in food distribution, oxygen and carbon dioxide concentrations, small molecule metabolites and others (Calhoun et al., 2015; Carrillo and Hallem, 2015; Ludewig and Schroeder, 2013). To uncouple the tactile and chemosensory input of the bacteria [*C. elegans* consume *E. coli* (Brenner, 1974)] from the nutritional value of ingesting bacteria, we analyzed the effect of modified bacteria on animal behavior. Aztreonam is a drug that inhibits bacterial cell wall synthesis and results in long filaments of bacteria that do not divide and cannot pass through the grinder into the *C. elegans* intestine (Gruninger et al., 2008). Animals exposed to aztreonam-treated bacteria experience the tactile and chemosensory input, but are unlikely to derive nutritional value from the food. We found that exposing animals to drug-treated bacteria for 3 hours was sufficient to reduce their sensitivity to copper, suggesting that the lack of food in the animal alters copper sensitivity (Figure 1F). Together, these results show that the lack of food in the *C. elegans* intestine, but not the absence of sensory cues, reduces the animal's sensitivity to copper.

Food deprivation reduces reorientations enabling more animals to cross the repellent barrier

To analyze how food deprivation modifies animal behavior, we developed a new multi-worm tracker. This tracker enables us to identify individual animals and their trajectories over many minutes as they integrate repellent and attractant signals in the sensory integration assay (see

Extended Experimental Procedures for details of the tracker). We tracked animals in both well-fed and food-deprived conditions and filtered the tracking data to consider a time window between 3 and 15 minutes in the assay. Additionally, we included events executed by animals moving towards the copper barrier. We found that food-deprived animals are more likely to cross the repellent barrier when compared to well-fed animals as shown by the increased density of well-fed animal tracks before the copper barrier (Figure 2A, 2B). We performed a similar analysis on animals moving away from the copper barrier and found no significant differences between well-fed and food-deprived conditions (data not shown). We then fit a Laplace mixture model for the distribution of turn events observed at different distances from the copper barrier (Figure S3A-D). This allows us to precisely quantify the reorientations and small turns as the animals approached the copper barrier and after crossing the barrier (see Extended Experimental Procedures for quantification details). While a large reorientation allows the animal to reverse its direction of movement, small turns generate smaller changes in the direction (Figure S3A-D). These large reorientations and small turns are similar to the previously described "pirouettes" and "small turns" respectively (Iino and Yoshida, 2009; Pierce-Shimomura et al., 1999). Compared to food-deprived animals, we found that well-fed animals make significantly more reorientations as they approach the copper barrier (Figure 2C). In contrast, there is no difference between well-fed and food-deprived animals in their relative small turn probabilities (Figure 2D). Since our assays included a paralytic, we were unable to obtain movement data from animals close to diacetyl. Together, these results suggest that well-fed animals reorient more, thus avoiding the copper barrier, while food-deprived animals reorient less and cross the copper barrier more frequently. Moreover, these data also suggest that food-deprived animals are unlikely to avoid toxic copper compounds in their environment allowing them to execute food search strategies with higher risk.

Intestine and body wall muscles use MML-1, but not MXL-2 to sense the lack of food and releases peptides to signal to the neurons

Our studies show that the lack of food inside the animal is responsible for the transient reduction in copper sensitivity. We hypothesized that internal tissues sense this lack of food and signal to the nervous system to modify neuronal function and behavior. To gain insights into how these tissues sense the absence of food, we used a candidate gene approach. In mammalian cells,

glucose is rapidly converted to glucose-6-phostphate, whose levels are sensed by a two basic-helix-loop-helix-leucine zipper transcription factors, MondoA and ChREBP (Carbohydrate Response Element Binding Protein). In well-fed conditions, MondoA binds the excess glucose-6-phosphate and Mlx (Max-like protein X) and translocates to the nucleus where it activates transcription of glucose-responsive genes. In the absence of glucose, MondoA remains in the cytoplasm (Havula and Hietakangas, 2012; Stoltzman et al., 2008). *C. elegans* homologs for MondoA and Mlx have been identified as MML-1 and MXL-2 respectively (Grove et al., 2009). Furthermore, MML-1 has also been shown to translocate into the intestinal nuclei under well-fed conditions (Johnson et al., 2014). We predicted that *mml-1* mutants would be unable to sense the lack of food and thereby unable to reduce copper sensitivity after food deprivation. Consistently, we found that *mml-1*, but not *mxl-2* mutants are defective in their integration responses after food deprivation (Figure 3A). To localize the MML-1 function to a specific tissue, we expressed the full-length coding sequence under specific promoter elements and analyzed its effect on behavior. We used promoter elements that drive expression in all neurons (*H20*), intestine (*gly-19*) or body wall muscles (*myo-3*) (Figure 3B) (Okkema et al., 1993; Shioi et al., 2001; Warren et al., 2001). We find that expressing the full-length cDNA encoding MML-1 specifically in the intestine and body wall muscles, but not neurons is sufficient to restore normal behavior to *mml-1* mutants (Figure 3A). We suggest that in the absence of food, MML-1 remains in the cytoplasm of intestinal and body wall muscle cells and speculate that the cytosolic MML-1 reduces copper sensitivity by modifying signaling between tissues.

Next, we hypothesized that the intestine and body wall muscles release peptide signals to relay the lack of food signal to the nervous system. To identify the relevant class of peptides, we analyzed gene mutants in peptide processing. The *C. elegans* genome encodes four known pro-protein covertases (AEX-5, EGL-3, BLI-4, and KPC-1) that cleave an overlapping subset of pro-peptides to generate mature peptides, which are further modified and packed into dense core vesicles (Li and Kim, 2008). Upon activation, dense core vesicles are released using the CAPS protein (calcium activated protein for secretion, *unc-31*) (Figure 3C) (Speese et al., 2007). We found that *aex-5* mutants were specifically defective in their sensory integration response under food-deprived, but not well-fed condition (Figure 3D, Table S1). In contrast, *egl-3* mutants were defective in their sensory integration behavior in both well-fed and food-deprived conditions,

while *bli-4* and *kpc-1* were defective only in the well-fed state (Figure 3D and Table S1). Previously, neuropeptide signaling has been shown to play a role in modifying sensory integration behavior (Ishihara et al., 2002) and we suggest that peptides processed by EGL-3, BLI-4 and KPC-1 might be involved. Together these results show that AEX-5-processed peptides are specifically required for animals to reduce their copper sensitivity after food deprivation.

To localize AEX-5 function to a specific tissue, we expressed the full-length coding sequence under specific promoter elements that drive expression in all neurons (*unc-119*), intestine (*gly-19*), body wall muscles (*myo-3*), pharynx (*myo-2*) and tail (*lin-44*) in the null mutant background and analyzed its effects on behavior (Figure 3B) (Hilliard and Bargmann, 2006; Maduro and Pilgrim, 1995; Okkema et al., 1993; Warren et al., 2001). We found that restoring AEX-5 to either the intestine, body wall muscles or neurons but not the pharynx or tail was sufficient to revert *aex-5* null mutants to normal modulation after food deprivation (Figure 3E). To confirm AEX-5 function in intestine, body wall muscles and neurons, we knocked down this gene specifically in those tissues and analyzed the effects on integration behavior. Expressing sense and anti-sense transcripts under cell-selective promoters has been shown to knock down the gene of interest in the target cells (Esposito et al., 2007; Leinwand and Chalasani, 2013). Using this approach, we found that knocking down *aex-5* in the intestine, body wall muscles or neurons generated animals that were defective in altering behavior after food-deprivation (Figure 3F). Previously, AEX-5 was shown to function in the intestine to modulate defecation behavior and body wall muscles to affect neuromuscular junction function (Mahoney et al., 2008; Sheng et al., 2015). However, our results showing AEX-5 activity in neurons are novel. Also, we found that knocking down UNC-31 [CAPS protein required for peptide release (Speese et al., 2007)] in the intestine, body wall muscles or neurons also rendered animals unable to modify their response in the integration assay after food deprivation (Figure 3G). Taken together, these results suggest that while AEX-5 processing is required in the intestine, body wall muscles and neurons, release of AEX-5 processed peptides from any of those tissues is sufficient to reduce copper sensitivity after food deprivation. Moreover, our results also show that the intestine and body wall muscles also use dense core vesicles to release peptides, a novel mechanism.

ASI chemosensory neurons use DAF-2 receptors to integrate intestine-released AEX-5 processed peptide(s)

To gain insights into the nature of the intestine-released peptide signal, we analyzed mutants in downstream receptors. The *C. elegans* genome encodes at least 122 neuropeptide genes including 42 neuropeptide like proteins (NLPs), FMRFamine-related peptides (FLPs) and 40 insulin-like peptides (ILPs) (Hobert, 2013). Many of the NLPs and FLPs are thought to act on G-protein coupled receptors (GPCRs), while ILPs bind the receptor tyrosine kinase, DAF-2 to influence cellular functions (Chen et al., 2013b; Hobert, 2013; Leinwand and Chalasani, 2013; Pierce et al., 2001). Upon binding cognate ligand(s), GPCRs use heterotrimeric Gαβγ proteins to activate signal transduction (Hamm, 1998). There are two Gγ subunits, *gpc-1* and *gpc-2* in the *C. elegans* genome, both with viable null mutants (Jansen et al., 1999). We found that mutants in the insulin receptor, DAF-2, were defective in their response to food deprivation, suggesting that the intestine and other tissues might release insulin-like peptide(s) to modify integration response after food deprivation (Figure 4A). In contrast, mutants in the two Gγ subunits or the carboxypeptidase, EGL-21, which is required to generate mature NLPs and FLPs (Husson et al., 2007) are not defective in their responsivity to copper after food deprivation (Figure S4A). Together, these data suggest that insulin signaling might be involved in reducing copper sensitivity after food deprivation.

To localize the site of DAF-2 action, we analyzed the effect of rescuing this receptor in different tissues. We found that expressing *daf-2* under the neuronal, but not intestine or body wall muscle promoters (Hung et al., 2014) restored normal behavior to the *daf-2* mutants (Figure 4A). These results implied that AEX-5 convertase might process an insulin-like peptide(s) in the various internal tissues. To identify the cognate ligand(s), we analyzed null mutants or RNA interference knockdowns against each of the 40 insulin-like peptides (Hobert, 2013). However, we found that none of the gene mutants or knockdowns in these peptides affected the altered integration response upon food deprivation (Table S2). We speculate that a combination of insulin-like or other peptide(s) might relay the lack of food signal from the intestine and other tissues. Taken together, these results suggest that neuronally expressed DAF-2 receptors might detect AEX-5 processed peptides that are released from multiple internal tissues.

To localize DAF-2 function to individual neurons, we used cell-selective promoters and generated transgenic animals. Previous studies have shown that three pairs of chemosensory neurons ASI, ASH and ADL detect copper ions and generate avoidance response (Hilliard et al., 2002). Given that food deprivation alters the animal's response to copper ions specifically, we tested whether DAF-2 was required in any of these sensory neurons. We found that restoring DAF-2 to ASI, but not ASH or ADL was sufficient to restore normal behavior to *daf-2* mutants (Figure 4B, Table S1). ASI-specific expression does not completely rescue the food-deprivation driven *daf-2* mutant behavioral phenotype suggesting that DAF-2 might also be required in additional neurons. Together, these results suggest that ASI neurons use DAF-2 receptors to detect internal tissue-released peptide(s) to modify integration behavior.

ASI neurons use non-canonical insulin signaling to integrate AEX-5 processed peptide signals

To identify the components of the DAF-2 signaling in ASI neurons that integrate food status signals, we analyzed gene mutants in candidate pathway components (Figure 4C). We observed that mutants in the canonical insulin-signaling pathway components phosphoinositide 3-kinase (PI3K, *age-1*), serine/threonine kinases AKT-1, AKT-2 (*akt-1*, *akt-2*), 3-phosphoinositide-dependent kinase 1 (*pdk-1*) and lipid phosphatase (*daf-18*, PTEN suppressor) performed normally in the sensory integration assay after food deprivation (Figure S4B) (Lapierre and Hansen, 2012). In contrast, mutants in serum and glucocorticoid inducible kinase-1 (*sgk-1*) are defective in their copper sensitivity after food deprivation (Figure 4D). We found that restoring SGK-1 function to ASI neurons specifically was sufficient for normal integration response in food-deprived *sgk-1* mutants (Figure 4D). SGK-1 has been previously shown to interact with the mTORC2 complex including Rictor (Jones et al., 2009; Mizunuma et al., 2014). We also tested mutants in *rict-1* (*C. elegans* Rictor) in our sensory integration assay and found that these mutants are also unable to alter their behavior after food deprivation (Figure 4D). Similar to SGK-1, we found that RICT-1 was also required in ASI neurons to restore normal food-deprivation behavior to *rict-1* mutants (Figure 4D). These results suggest that SGK-1 and RICT-1 might function in the same pathway downstream of DAF-2 receptors in ASI neurons. These results are consistent with previous studies showing that SGK-1 and mTORC2 act parallel to the

canonical insulin-signaling pathway to regulate stress responses and animal lifespan (Hertweck et al., 2004). Collectively, these results show that both SGK-1 and RICT-1 function in ASI neurons downstream of DAF-2 receptors to reduce copper sensitivity after food deprivation.

To test whether AEX-5 and DAF-2 function in the same pathway, we performed genetic epistasis experiments. We generated an *aex-5;daf-2* double mutant, which did not show any additional defects when compared to either *aex-5* or *daf-2* single mutant (Figure 4E). We also found that expressing AEX-5 in the intestine and DAF-2 in ASI sensory neurons restored normal integration response after food deprivation (Figure 4E). Together, these data show that the intestine released AEX-5 processed peptides are detected by ASI neurons using the DAF-2 receptors. These results suggest the following order for these signaling events: food deprivation leads to lack of food within the animal, which is detected by the intestine and body wall muscles using cytosolic MML-1 leading to the release of AEX-5 processed peptides that bind DAF-2 receptors and are processed by downstream SGK-1 and RICT-1 in ASI and other neurons to reduce copper sensitivity and alter behavior.

Food-deprivation alters ASI neuronal adaptation rate

To test how food deprivation modifies neural function, we probed the activity of copper-sensitive neurons using calcium imaging. We localized a genetically encoded calcium indicator (Akerboom et al., 2012) to the nuclei of ASI and ASH neurons, allowing us to measure neural activity in both neurons simultaneously. We also expressed the fluorescent mCherry protein under an ASI-selective promoter in the same transgenic animal enabling us to specifically identify ASI neuronal nuclei (Figure S5A-C). Recently, nuclear calcium dynamics have been shown to be similar to those measured from the cytoplasm (Schrodel et al., 2013), validating our approach. We presented the repellent copper solution to the nose of an animal constrained in a microfluidic device and recorded neural activity as previously described (Chalasani et al., 2007) in both well-fed and food-deprived conditions. We found that both well-fed and food-deprived animals responded similarly to long pulses (30 seconds) of repellent stimuli (data not shown). We then presented the repellent stimulus as 1-second pulses (1 second on, 1 second off) for 30 seconds. This protocol allows us to probe the activity of ASI and ASH neurons to repeated pulses of copper solution, a regimen that animals might experience as they encounter the copper

barrier (see Experimental Procedures). We found that well-fed ASI neurons responded to the removal of copper stimuli with increasing fluorescence changes until a maximal fluorescence change (peak). Subsequently, the ASI calcium signals dropped suggesting that this neuron had adapted to the copper stimuli (black line indicates average, Figure 5A). This result is consistent with previous studies showing that adapted chemosensory neurons do not respond to stimuli (Chalasani et al., 2010). In contrast, under food-deprived conditions, ASI neurons had a higher threshold requiring additional stimulus pulses to observe a calcium change. Moreover, we did not observe a distinct maximal fluorescence or a decline in the calcium signal, suggesting that ASI neurons did not adapt (green line indicates average, Figure 5A). Moreover, in both well-fed and food-deprived conditions, we observe an ASI calcium response to the removal of last copper stimulus suggesting that there are additional calcium dynamics. Given that we observe food-deprivation modifies animal behavior as the animal experiences the copper barrier, we focused our analysis on the calcium dynamics obtained in response to the repeated stimuli. We quantified the average change in fluorescence in an 8-second window both before and after the peak in well-fed conditions and compared the data to a similar time window in the food-deprived conditions (Figure 5B). We also tested ASI responses to additional copper stimulus concentrations and observed similar dynamics at 25 mM and 100 mM, but not at 10 mM (Figure S6A, S6C and S6E). These data suggest that ASI neurons show a dose-dependent response to the removal of copper stimuli and can adapt to repeat stimulus pulses, which is altered by food deprivation. Together, these data show that food deprivation increases the stimulus threshold and transforms ASI from an adapting to a non-adapting state.

Next, we analyzed ASH activity data in both well-fed and food-deprived conditions. We found that ASH neurons responded to both the addition and removal of copper stimuli. Under well-fed conditions, we observed complex dynamics including an increase in calcium signal to the initial stimulus pulses followed by responses without change in baseline through the middle stimulus pulses and finally, a smaller decline in the baseline response to the last few stimulus pulses (black line indicates average, Figure 5C). We also find that food deprivation lowers the ASH threshold (higher response to the initial stimulus pulses), which is followed by responses without change in baseline through the middle stimulus pulses and no decline in the baseline response to the last few stimulus pulses (green line indicates average, Figure 5C). Similar to ASI

dynamics, we also observe ASH responses to removal of the last copper stimulus pulses suggesting additional dynamics. We performed a similar analysis on the ASH calcium data and found that food deprivation reduces the stimulus threshold and had a smaller effect on the ASH adaptation rate (Figure 5D). We also tested additional copper stimulus concentrations and found that ASH neurons also show dose-dependent responses to both addition and removal, but are not significantly affected by food deprivation. Together, these data show that food deprivation reduces the stimulus threshold of ASH neurons and likely affects additional stimulus dynamics.

Our genetic experiments showed that food-deprivation effects are lost in *daf-2* mutants. To test whether the changes in ASI neural activity also use the same genetic pathway, we performed a similar analysis of their copper-evoked responses in *daf-2* mutants. Consistent with our genetic analysis, we found that the ASI-specific neural activity changes after food deprivation are lost in the *daf-2* mutants (Figure 6A-6D). We also compared the ratio of change in food-deprived to well-fed conditions in both wild-type and *daf-2* mutants and found that the insulin-receptor mutant had a significant effect on ASI, but not ASH activity (Figure 6E). Collectively, these results show that food deprivation affects ASI threshold and adaptation kinetics in a DAF-2 dependent manner.

Discussion

We used food deprivation in *C. elegans* as a model to understand how changes in internal states modify behavior. We show that food-deprived animals reversibly alter their behavior by reducing their repellent responsiveness, allowing them to traverse potentially toxic environments in their search for food. Multiple tissues including the intestine, body wall muscles and neurons independently sense the lack of food and release peptide signals that are integrated by DAF-2 receptors on ASI neurons (Figure 6F). This novel, non-neuronal, dense core vesicle release dependent peptide signaling transforms ASI neurons from a rapidly adapting to a non-adapting neuron modifying animal behavior. We suggest that altering the state of sensory neurons affords greater dynamic range of control over behavioral decisions. More generally, we demonstrate how neuronal activity is regulated by internal state signals to modify behaviors lasting many minutes.

Multiple tissues release peptide(s) to signal “lack of food”

Multicellular animals sense and regulate glucose homeostasis at several levels. While insulin and glucagon maintain constant levels of circulating glucose, the Myc-family transcription factors are used within cells. Glucose uses cell-membrane localized transporters to enter cells, where it is rapidly converted into glucose-6-phosphate (Jordan et al., 2010). This intermediate metabolite is sensed by the Myc-Max complex, which binds glucose-6-phosphate and translocates to the nucleus where it regulates the transcription of glucose-responsive genes (Havula and Hietakangas, 2012). While the role of ChREBP/MondoA-Mlx-glucose-6-phosphate complex in regulating the gene transcription is well studied (Li et al., 2010; Stoeckman et al., 2004; Stoltzman et al., 2008), the role of these proteins in the cytoplasm remains poorly understood. We show a specific role for MML-1 (MondoA homolog), but not MXL-2 (Mlx homolog) in the intestine and body wall muscles in reducing copper sensitivity after food deprivation. We suggest that in the absence of MML-1, these two tissues are unable to detect the lack of glucose and do not relay signals to modify the downstream neuronal circuits. Moreover, we also speculate that MML-1 (MondoA) accumulation in the cytoplasm (in the absence of glucose) enables the intestine and body wall muscle cells to release peptide(s) relaying a “lack of glucose” signal to other tissues.

Our analysis describes a role for the pro-protein convertases in modifying behavior upon food deprivation. We show that while *egl-3, bli-4* and *kpc-1* mutants are defective in their sensory integration response, *aex-5* mutants are specifically affected in their response to food deprivation. Moreover, we show that AEX-5 functions in the intestine, body wall muscles and neurons to process relevant peptide(s). Previously, *aex-5* has been shown to function in both the body wall muscle cells and the intestine to regulate exocytosis at the neuromuscular junction and the defecation motor program respectively (Doi and Iwasaki, 2002; Sheng et al., 2015). However, our studies confirming a role for AEX-5 in neurons are novel. We suggest that *C. elegans* neurons use a MML-1 independent mechanism to detect the lack of glucose and release AEX-5 processed peptide(s). Surprisingly, we find that restoring AEX-5 function to the intestine, the body wall muscles or neurons is sufficient to restore normal behavior to *aex-5* mutants, while knocking down this gene in any of these three tissues disrupts wild-type behavior. Together, these results suggest that intestine, body wall muscle or neuronal release of AEX-5 processed peptide(s) alone is sufficient to relay food status signals and this signaling is required in all three

tissues in wild-type animals. Given that our transgenic rescue experiments involve expressing more than one copy of the AEX-5 protease in the three tissues (see Extended Experimental Procedures), we speculate that this "food status" signaling is regulated at the level of pro-peptide cleavage such that excess mature peptide(s) from the intestine, body wall muscles or neurons can compensate for the lack of signal from the other two tissues.

Moreover, we also identify a role for the dense core vesicle release machinery in non-neuronal tissues including the intestine and body wall muscles. Interestingly, in mammals a second CAPS protein (CAPS2) that is expressed in non-neuronal tissues has been identified (Speidel et al., 2003). These results suggest that peptide release from non-neuronal tissues might also involve dense core vesicles across multiple species from worms to mammals. Collectively, we show that multiple tissues including the intestine, body wall muscles and neurons process precursors using the AEX-5 protease and release mature peptide(s) using the CAPS protein relaying "food status" signals to downstream neurons.

ASI chemosensory neurons integrate "food status" signals

Our studies show that while the intestine, body wall muscles and neurons release AEX-5 processed peptide(s), ASI chemosensory neurons use the tyrosine kinase insulin receptor (DAF-2) to integrate these signals. Three lines of evidence suggest that the internal tissues are releasing insulin-like peptide(s)- first, the food-deprivation effect does not require G-protein receptor signaling, second, the insulin receptor (DAF-2) integrates these signals and third, DAF-2 and AEX-5 function in the same pathway. Although our efforts to identify the cognate insulin-like peptide (ILP) have been unsuccessful, we suggest that combination of ILPs might relay "food status" signals from the intestine, body wall muscles and neurons to ASI sensory neurons. We also find that non-canonical signaling pathway components are used downstream of DAF-2 to integrate these peptide signals. Our results show that while PI-3Kinase, AKT kinase -1 and -2, PDK-1 and PTEN are not required, SGK-1 (serum and glucocorticoid inducible kinase) and its binding partner Rictor (a component of the mTORC2 complex) are required to integrate AEX-5 processed peptide signals. Although SGK-1 has been shown to phosphorylate DAF-16 (FOXO) in vitro (Hertweck et al., 2004), it might also indirectly regulate a subset of the DAF-16 target genes (Chen et al., 2013a; Murphy and Hu, 2013). We suggest that this SGK-1-Rictor

(mTORC2) complex might integrate signals from multiple pathways including DAF-2 signaling to regulate DAF-16-target genes (Mizunuma et al., 2014) and modify neuronal functions and animal behavior.

Our genetic analysis shows that ASI chemosensory neurons integrate peptide signals and modify integration response after food deprivation. ASI neurons have been previously shown to detect food signals to modify animal behavior (Calhoun et al., 2015; Gallagher et al., 2013). However, our results showing that ASI integrates internal food status signals are novel.

Food-deprivation alters the ASI neural adaptation rate

Our imaging experiments show that ASH neurons respond to the copper pulses, before ASI neurons, suggesting that ASH might be a low-threshold, while ASI is a high-threshold copper detector. This is consistent with previous results showing that ASH is crucial for copper avoidance (Hilliard et al., 2005; Hilliard et al., 2002) and with data showing that ASI is a high-threshold detector for food (Calhoun et al., 2015). This dual coding strategy with high and low-threshold neurons is commonly used across *C. elegans* and others species to efficiently encode stimulus information (Calhoun et al., 2015; McGlone and Reilly, 2010). Moreover, our analysis of ASH and ASI neural activity in *daf-2* mutants reveals a surprising feature. We find that ASH responses are greatly reduced in the *daf-2* mutants, but spare some neural dynamics, particularly in the early stimulus pulses. In contrast, the dynamics of the high-threshold ASI neurons are significantly altered. We suggest that the food-deprivation signal has a stronger influence on the high-threshold ASI, while sparing some of the signaling from the low threshold ASH neurons. These results are also consistent with our genetic experiments showing that DAF-2 is specifically required in ASI, but not ASH neurons to integrate internal food status signals.

We also show that food deprivation alters the adaptation kinetics in ASI sensory neurons and reduces its responsiveness to copper stimuli. Adaptation is a fundamental property of many sensory systems, enabling neurons to extract relevant information from background noise (Mease et al., 2013; Wark et al., 2009). Sensory neurons have been shown to adapt to a variety of stimulus distributions and efficiently encode information (Wark et al., 2007). Indeed, individual neurons in the rodent sensorimotor cortex and retinal ganglion cells and others have been shown

to alter their input-output properties based on the size of the input stimulus and local statistical context (Mease et al., 2013; Wark et al., 2009). We observe a similar change in the ASI neural activity, where it adapts to repeated stimulus pulses allowing them to read local concentration gradients more effectively. In contrast, under food-deprived conditions, the adaptation rate is reduced making these neurons insensitive to changes in copper stimuli. Moreover, we also show that non-canonical insulin signaling mediates some aspects of food deprivation by altering neural adaptation rates leading to flexible behaviors. We suggest that similar peptide signaling pathways might exist across different animal species allowing their nervous systems to integrate internal information like food deprivation, stress and others.

We speculate that changes in ASI neuronal properties might underlie altered animal behavior. We observe that food-deprived animals have fewer reorientations as they approach the copper barrier allowing them cross the repellent and approach the attractant. In contrast, well-fed animals have higher number of reorientations allow them to avoid the copper barrier. We suggest that transforming ASI from a rapidly adapting to a non-adapting neuron prevents this neuron from detecting local changes in copper leading to fewer reorientations and allowing the food-deprived animals to cross the copper barrier. These data are also consistent with previous studies showing that ASI neurons suppress reorientations indicating that animals with high ASI activity will re-orient less (Gray et al., 2005). These studies link metabolite sensing by internal tissues with non-canonical insulin signaling that alters neuronal adaptation rate to modify chemosensory behavior, a mechanism likely conserved across species.

Experimental Procedures

Standard culture, molecular biology and injection methods were used; details and strain genotypes; tracker and calcium imaging data analysis are in Extended Experimental Procedures.

Behavior Assays

Control and food-deprived animals were grown to adulthood on regular nematode growth medium (NGM) plates before they were washed and transferred to new food or food-free plates respectively for the indicated duration. Sensory integration assay was performed on 2% agar plates containing 5mM potassium phosphate (pH 6), 1mM $CaCl_2$ and 1mM $MgSO_4$. Repellent

gradients (including $CuSO_4$, glycerol, NaCl, and quinine) were established by dripping 25µl of solution across the midline of the plate (Ishihara et al., 2002). Copper gradients were visualized using dyes (see Extended Experimental Procedures). Prior to the assay, the animals were washed from the food or food-free plates before being transferred to the assay plates. After 45 minutes or at indicated times, the integration index was computed as the number of worms in the odor half of the plate minus the worms in origin half of the plate divided by the total number of worms that moved beyond the origin. The percent increase of food-deprived animals from well-fed controls was calculated by subtracting the averaged well-fed integration indices from each food-deprived integration index, divided by the averaged well-fed integration index. Nine or more assays were performed on at least three different days. Two-tailed unpaired *t* tests (for Figure 1B only) and one sample *t* tests were used to obtain statistical information across food conditions. An ordinary one-way ANOVA test was used to compare all conditions in Figures 1D –E. To compare across strains for genetic rescue or knock down experiments, unpaired *t* test with Welch's correction was used.

Aztreonam-treated bacteria were prepared as previously described (Gruninger et al., 2008). *E. coli* was grown at 37°C overnight while shaking vigorously to an optical density (OD) of less than 0.6 to avoid log phase. This culture was treated with aztreonam antibiotic (Sigma) at a final concentration of 10 µg/ml and incubated at 37°C for 3 hours with minimal shaking at 70 RPM. Aztreonam-treated bacteria were immediately spread on plates also with 10 µg/ml aztreonam, dried and used that day for behavior experiments.

Calcium Imaging

C. elegans expressing nuclear-localized GCaMP5K calcium indicators (Akerboom et al., 2012) under an ASH and ASI selective promoter are trapped and imaged using a PDMS based microfluidic device (Chalasani et al., 2007). Expressing mCherry protein in the cytoplasm under an ASI-specific promoter identified ASI neurons. Both ASI and ASH neurons were imaged simultaneously. M13 buffer (30mM Tris-HCl pH 7.0, 100mM NaCl and 10 mM KCl) were used in all imaging experiments to prevent $CuSO_4$ from precipitating. Prior to data collection, ASH neurons were exposed to blue light for two minutes as previously published (Hilliard et al., 2005). Each animal was only imaged once using the 1-second on, 1-second off pulse protocol. Images were captured using Metamorph software on an inverted microscope using a

Photometrics EMCCD camera. Baseline F_0 was measured as average fluorescence during a three-second window (1s-4.4s). The ratio of change in fluorescence to the baseline F_0 is plotted using custom MATLAB scripts.

Fat quantification

Oil red O staining was conducted as previously described (Soukas et al., 2009). Briefly, synchronized animals under well-fed or food-deprived animals were kept on ice for 10 minutes to stop pharyngeal activity. After fixation, animals were taken through three freeze-thaw cycles and exposed to a working solution of oil red O stain (40% water: 60% oil red O in isopropanol). Animals were imaged with a 20X objective on a Zeiss Axio Imager and an Orca Flash 4.0 camera. In all cases, staining in the intestine within 500 pixels from the bulb was quantified using ImageJ (NIH). Percent of stained pixels was calculated using ImageJ, which assigned every pixel a value on a gray scale of 0 (Black) – 255 (white), values of less than 50 correspond to staining. We estimated a ratio by calculating the sum of these 50 pixels and dividing it by the total number of pixels (150,000 pixels). Within each experiment, 14 animals from each condition were quantified and all experiments were repeated at least three times on different days. Data were analyzed for significance using Student's *t* test and error bars represent SEM.

Author Contributions

H.E.L. conceived and conducted the experiments, interpreted the data, and co-wrote the paper. Z.T.C wrote the tracker program, analyzed the tracking data, and co-wrote the paper. Z. L. and C.J.Y. conducted behavioral assays. T.O.S. interpreted the data and provided guidance for the data analysis. S.H.C. conceived the experiments, interpreted the data and co-wrote the paper.

Acknowledgements

We thank A. Dillin, T. Ishihara, S. Lockery, A. Samuelson, E. Troemel, M. Zhen, the National BioResource Project (NBRP, Japan) and Caenorhabditis Genetics Center (CGC) for strains; C. Bargmann, E. Hallem, M. Hilliard, A. van der Linden, P. McGrath, D. Pilgrim and P. Sengupta for constructs; S. Srinivasan and lab members for RNAi clones and help with oil red O staining. We are also grateful to L. Stowers, J. Wang, S. Asinof, L. Hale, U. Magaram, L. Shipp, K. Quach, C. Yeh and members of the Chalasani lab for critical comments, advice, and insights.

This work was funded by grants from The Rita Allen Foundation, The W.M. Keck Foundation and NIH R01MH096881-03 to S.H.C. H.E.L. was initially supported by the Socrates Program funded by NSF GK-12 STEM Fellows in Education (Award #NSF-742551) followed by a Graduate Research Fellowship also from the NSF.

References

Air, E.L., Benoit, S.C., Clegg, D.J., Seeley, R.J., and Woods, S.C. (2002). Insulin and leptin combine additively to reduce food intake and body weight in rats. Endocrinology *143*, 2449-2452.

Akerboom, J., Chen, T.W., Wardill, T.J., Tian, L., Marvin, J.S., Mutlu, S., Calderon, N.C., Esposti, F., Borghuis, B.G., Sun, X.R., *et al.* (2012). Optimization of a GCaMP calcium indicator for neural activity imaging. J Neurosci *32*, 13819-13840.

Andrews, Z.B., Liu, Z.W., Walllingford, N., Erion, D.M., Borok, E., Friedman, J.M., Tschop, M.H., Shanabrough, M., Cline, G., Shulman, G.I., *et al.* (2008). UCP2 mediates ghrelin's action on NPY/AgRP neurons by lowering free radicals. Nature *454*, 846-851.

Atasoy, D., Betley, J.N., Su, H.H., and Sternson, S.M. (2012). Deconstruction of a neural circuit for hunger. Nature *488*, 172-177.

Avery, L. (1993). The genetics of feeding in Caenorhabditis elegans. Genetics *133*, 897-917.

Avery, L., and Horvitz, H.R. (1990). Effects of starvation and neuroactive drugs on feeding in Caenorhabditis elegans. J Exp Zool *253*, 263-270.

Berthoud, H.R. (2011). Metabolic and hedonic drives in the neural control of appetite: who is the boss? Curr Opin Neurobiol *21*, 888-896.

Brenner, S. (1974). The genetics of Caenorhabditis elegans. Genetics *77*, 71-94.

Calhoun, A.J., Tong, A., Pokala, N., Fitzpatrick, J.A., Sharpee, T.O., and Chalasani, S.H. (2015). Neural Mechanisms for Evaluating Environmental Variability in Caenorhabditis elegans. Neuron *86*, 428-441.

Carlini, V.P., Varas, M.M., Cragnolini, A.B., Schioth, H.B., Scimonelli, T.N., and de Barioglio, S.R. (2004). Differential role of the hippocampus, amygdala, and dorsal raphe nucleus in regulating feeding, memory, and anxiety-like behavioral responses to ghrelin. Biochem Biophys Res Commun *313*, 635-641.

Carrillo, M.A., and Hallem, E.A. (2015). Gas sensing in nematodes. Mol Neurobiol *51*, 919-931.

Chalasani, S.H., Chronis, N., Tsunozaki, M., Gray, J.M., Ramot, D., Goodman, M.B., and Bargmann, C.I. (2007). Dissecting a circuit for olfactory behaviour in Caenorhabditis elegans. Nature *450*, 63-70.

Chalasani, S.H., Kato, S., Albrecht, D.R., Nakagawa, T., Abbott, L.F., and Bargmann, C.I. (2010). Neuropeptide feedback modifies odor-evoked dynamics in Caenorhabditis elegans olfactory neurons. Nat Neurosci *13*, 615-621.

Chen, A.T., Guo, C., Dumas, K.J., Ashrafi, K., and Hu, P.J. (2013a). Effects of Caenorhabditis elegans sgk-1 mutations on lifespan, stress resistance, and DAF-16/FoxO regulation. Aging Cell *12*, 932-940.

Chen, Z., Hendricks, M., Cornils, A., Maier, W., Alcedo, J., and Zhang, Y. (2013b). Two insulin-like peptides antagonistically regulate aversive olfactory learning in C. elegans. Neuron *77*, 572-585.

Cowley, M.A., Smith, R.G., Diano, S., Tschop, M., Pronchuk, N., Grove, K.L., Strasburger, C.J., Bidlingmaier, M., Esterman, M., Heiman, M.L., *et al.* (2003). The distribution and mechanism of action of ghrelin in the CNS demonstrates a novel hypothalamic circuit regulating energy homeostasis. Neuron *37*, 649-661.

de Bono, M., and Bargmann, C.I. (1998). Natural variation in a neuropeptide Y receptor homolog modifies social behavior and food response in C. elegans. Cell *94*, 679-689.

Dietrich, M.O., and Horvath, T.L. (2012). Limitations in anti-obesity drug development: the critical role of hunger-promoting neurons. Nat Rev Drug Discov *11*, 675-691.

Dietrich, M.O., and Horvath, T.L. (2013). Hypothalamic control of energy balance: insights into the role of synaptic plasticity. Trends Neurosci *36*, 65-73.

Dietrich, M.O., Zimmer, M.R., Bober, J., and Horvath, T.L. (2015). Hypothalamic Agrp neurons drive stereotypic behaviors beyond feeding. Cell *160*, 1222-1232.

Doi, M., and Iwasaki, K. (2002). Regulation of retrograde signaling at neuromuscular junctions by the novel C2 domain protein AEX-1. Neuron *33*, 249-259.

Esposito, G., Di Schiavi, E., Bergamasco, C., and Bazzicalupo, P. (2007). Efficient and cell specific knock-down of gene function in targeted C. elegans neurons. Gene *395*, 170-176.

Ezcurra, M., Tanizawa, Y., Swoboda, P., and Schafer, W.R. (2011). Food sensitizes C. elegans avoidance behaviours through acute dopamine signalling. Embo J *30*, 1110-1122.

Figlewicz, D.P., and Sipols, A.J. (2010). Energy regulatory signals and food reward. Pharmacol Biochem Behav *97*, 15-24.

Gallagher, T., Kim, J., Oldenbroek, M., Kerr, R., and You, Y.J. (2013). ASI regulates satiety quiescence in C. elegans. J Neurosci *33*, 9716-9724.

Gillette, R., Huang, R.C., Hatcher, N., and Moroz, L.L. (2000). Cost-benefit analysis potential in feeding behavior of a predatory snail by integration of hunger, taste, and pain. Proc Natl Acad Sci U S A *97*, 3585-3590.

Gray, J.M., Hill, J.J., and Bargmann, C.I. (2005). A circuit for navigation in Caenorhabditis elegans. Proc Natl Acad Sci U S A *102*, 3184-3191.

Grove, C.A., De Masi, F., Barrasa, M.I., Newburger, D.E., Alkema, M.J., Bulyk, M.L., and Walhout, A.J. (2009). A multiparameter network reveals extensive divergence between C. elegans bHLH transcription factors. Cell *138*, 314-327.

Gruninger, T.R., Gualberto, D.G., and Garcia, L.R. (2008). Sensory perception of food and insulin-like signals influence seizure susceptibility. PLoS Genet *4*, e1000117.

Hamm, H.E. (1998). The many faces of G protein signaling. J Biol Chem *273*, 669-672.

Havula, E., and Hietakangas, V. (2012). Glucose sensing by ChREBP/MondoA-Mlx transcription factors. Semin Cell Dev Biol *23*, 640-647.

Hertweck, M., Gobel, C., and Baumeister, R. (2004). C. elegans SGK-1 is the critical component in the Akt/PKB kinase complex to control stress response and life span. Dev Cell *6*, 577-588.

Hilliard, M.A., Apicella, A.J., Kerr, R., Suzuki, H., Bazzicalupo, P., and Schafer, W.R. (2005). In vivo imaging of C. elegans ASH neurons: cellular response and adaptation to chemical repellents. Embo J *24*, 63-72.

Hilliard, M.A., and Bargmann, C.I. (2006). Wnt signals and frizzled activity orient anterior-posterior axon outgrowth in C. elegans. Dev Cell *10*, 379-390.

Hilliard, M.A., Bargmann, C.I., and Bazzicalupo, P. (2002). C. elegans responds to chemical repellents by integrating sensory inputs from the head and the tail. Curr Biol *12*, 730-734.

Hills, T., Brockie, P.J., and Maricq, A.V. (2004). Dopamine and glutamate control area-restricted search behavior in Caenorhabditis elegans. J Neurosci *24*, 1217-1225.

678 Hobert, O. (2013). The neuronal genome of Caenorhabditis elegans. WormBook, 1-106.
679 Hung, W.L., Wang, Y., Chitturi, J., and Zhen, M. (2014). A Caenorhabditis elegans
680 developmental decision requires insulin signaling-mediated neuron-intestine communication.
681 Development *141*, 1767-1779.
682 Husson, S.J., Janssen, T., Baggerman, G., Bogert, B., Kahn-Kirby, A.H., Ashrafi, K., and
683 Schoofs, L. (2007). Impaired processing of FLP and NLP peptides in carboxypeptidase E (EGL-
684 21)-deficient Caenorhabditis elegans as analyzed by mass spectrometry. J Neurochem *102*, 246-
685 260.
686 Iino, Y., and Yoshida, K. (2009). Parallel use of two behavioral mechanisms for chemotaxis in
687 Caenorhabditis elegans. J Neurosci *29*, 5370-5380.
688 Inagaki, H.K., Panse, K.M., and Anderson, D.J. (2014). Independent, reciprocal
689 neuromodulatory control of sweet and bitter taste sensitivity during starvation in Drosophila.
690 Neuron *84*, 806-820.
691 Ishihara, T., Iino, Y., Mohri, A., Mori, I., Gengyo-Ando, K., Mitani, S., and Katsura, I. (2002).
692 HEN-1, a secretory protein with an LDL receptor motif, regulates sensory integration and
693 learning in Caenorhabditis elegans. Cell *109*, 639-649.
694 Jansen, G., Thijssen, K.L., Werner, P., van der Horst, M., Hazendonk, E., and Plasterk, R.H.
695 (1999). The complete family of genes encoding G proteins of Caenorhabditis elegans. Nat Genet
696 *21*, 414-419.
697 Johnson, D.W., Llop, J.R., Farrell, S.F., Yuan, J., Stolzenburg, L.R., and Samuelson, A.V.
698 (2014). The Caenorhabditis elegans Myc-Mondo/Mad complexes integrate diverse longevity
699 signals. PLoS Genet *10*, e1004278.
700 Jones, K.T., Greer, E.R., Pearce, D., and Ashrafi, K. (2009). Rictor/TORC2 regulates
701 Caenorhabditis elegans fat storage, body size, and development through sgk-1. PLoS Biol *7*, e60.
702 Jordan, S.D., Konner, A.C., and Bruning, J.C. (2010). Sensing the fuels: glucose and lipid
703 signaling in the CNS controlling energy homeostasis. Cell Mol Life Sci *67*, 3255-3273.
704 Kawai, K., Sugimoto, K., Nakashima, K., Miura, H., and Ninomiya, Y. (2000). Leptin as a
705 modulator of sweet taste sensitivities in mice. Proc Natl Acad Sci U S A *97*, 11044-11049.
706 Kojima, M., Hosoda, H., Date, Y., Nakazato, M., Matsuo, H., and Kangawa, K. (1999). Ghrelin
707 is a growth-hormone-releasing acylated peptide from stomach. Nature *402*, 656-660.
708 Lapierre, L.R., and Hansen, M. (2012). Lessons from C. elegans: signaling pathways for
709 longevity. Trends Endocrinol Metab *23*, 637-644.
710 Leinwand, S.G., and Chalasani, S.H. (2013). Neuropeptide signaling remodels chemosensory
711 circuit composition in Caenorhabditis elegans. Nat Neurosci *16*, 1461-1467.
712 Li, C., and Kim, K. (2008). Neuropeptides. WormBook, 1-36.
713 Li, M.V., Chen, W., Harmancey, R.N., Nuotio-Antar, A.M., Imamura, M., Saha, P., Taegtmeyer,
714 H., and Chan, L. (2010). Glucose-6-phosphate mediates activation of the carbohydrate
715 responsive binding protein (ChREBP). Biochem Biophys Res Commun *395*, 395-400.
716 Lipton, J., Kleemann, G., Ghosh, R., Lints, R., and Emmons, S.W. (2004). Mate searching in
717 Caenorhabditis elegans: a genetic model for sex drive in a simple invertebrate. J Neurosci *24*,
718 7427-7434.
719 Ludewig, A.H., and Schroeder, F.C. (2013). Ascaroside signaling in C. elegans. WormBook, 1-
720 22.
721 Maduro, M., and Pilgrim, D. (1995). Identification and cloning of unc-119, a gene expressed in
722 the Caenorhabditis elegans nervous system. Genetics *141*, 977-988.

723 Mahoney, T.R., Luo, S., Round, E.K., Brauner, M., Gottschalk, A., Thomas, J.H., and Nonet,
724 M.L. (2008). Intestinal signaling to GABAergic neurons regulates a rhythmic behavior in
725 Caenorhabditis elegans. Proc Natl Acad Sci U S A *105*, 16350-16355.
726 Malik, S., McGlone, F., Bedrossian, D., and Dagher, A. (2008). Ghrelin modulates brain activity
727 in areas that control appetitive behavior. Cell Metab *7*, 400-409.
728 McGhee, J.D. (2007). The C. elegans intestine. WormBook, 1-36.
729 McGlone, F., and Reilly, D. (2010). The cutaneous sensory system. Neurosci Biobehav Rev *34*,
730 148-159.
731 Mease, R.A., Famulare, M., Gjorgjieva, J., Moody, W.J., and Fairhall, A.L. (2013). Emergence
732 of adaptive computation by single neurons in the developing cortex. J Neurosci *33*, 12154-
733 12170.
734 Mercer, R.E., Chee, M.J., and Colmers, W.F. (2011). The role of NPY in hypothalamic mediated
735 food intake. Front Neuroendocrinol *32*, 398-415.
736 Mizunuma, M., Neumann-Haefelin, E., Moroz, N., Li, Y., and Blackwell, T.K. (2014).
737 mTORC2-SGK-1 acts in two environmentally responsive pathways with opposing effects on
738 longevity. Aging Cell *13*, 869-878.
739 Moerman, D.G., and Williams, B.D. (2006). Sarcomere assembly in C. elegans muscle.
740 WormBook, 1-16.
741 Muller, T.D., Nogueiras, R., Andermann, M.L., Andrews, Z.B., Anker, S.D., Argente, J.,
742 Batterham, R.L., Benoit, S.C., Bowers, C.Y., Broglio, F., *et al.* (2015). Ghrelin. Molecular
743 metabolism *4*, 437-460.
744 Murphy, C.T., and Hu, P.J. (2013). Insulin/insulin-like growth factor signaling in C. elegans.
745 WormBook, 1-43.
746 Nassel, D.R., and Wegener, C. (2011). A comparative review of short and long neuropeptide F
747 signaling in invertebrates: Any similarities to vertebrate neuropeptide Y signaling? Peptides *32*,
748 1335-1355.
749 Okkema, P.G., Harrison, S.W., Plunger, V., Aryana, A., and Fire, A. (1993). Sequence
750 requirements for myosin gene expression and regulation in Caenorhabditis elegans. Genetics
751 *135*, 385-404.
752 Pierce, S.B., Costa, M., Wisotzkey, R., Devadhar, S., Homburger, S.A., Buchman, A.R.,
753 Ferguson, K.C., Heller, J., Platt, D.M., Pasquinelli, A.A., *et al.* (2001). Regulation of DAF-2
754 receptor signaling by human insulin and ins-1, a member of the unusually large and diverse C.
755 elegans insulin gene family. Genes Dev *15*, 672-686.
756 Pierce-Shimomura, J.T., Morse, T.M., and Lockery, S.R. (1999). The fundamental role of
757 pirouettes in Caenorhabditis elegans chemotaxis. J Neurosci *19*, 9557-9569.
758 Sawin, E.R., Ranganathan, R., and Horvitz, H.R. (2000). C. elegans locomotory rate is
759 modulated by the environment through a dopaminergic pathway and by experience through a
760 serotonergic pathway. Neuron *26*, 619-631.
761 Schrodel, T., Prevedel, R., Aumayr, K., Zimmer, M., and Vaziri, A. (2013). Brain-wide 3D
762 imaging of neuronal activity in Caenorhabditis elegans with sculpted light. Nat Methods *10*,
763 1013-1020.
764 Sengupta, P. (2013). The belly rules the nose: feeding state-dependent modulation of peripheral
765 chemosensory responses. Curr Opin Neurobiol *23*, 68-75.
766 Sheng, M., Hosseinzadeh, A., Muralidharan, S.V., Gaur, R., Selstam, E., and Tuck, S. (2015).
767 Aberrant fat metabolism in Caenorhabditis elegans mutants with defects in the defecation motor
768 program. PLoS One *10*, e0124515.

Shioi, G., Shoji, M., Nakamura, M., Ishihara, T., Katsura, I., Fujisawa, H., and Takagi, S. (2001). Mutations affecting nerve attachment of Caenorhabditis elegans. Genetics *157*, 1611-1622.

Soukas, A.A., Kane, E.A., Carr, C.E., Melo, J.A., and Ruvkun, G. (2009). Rictor/TORC2 regulates fat metabolism, feeding, growth, and life span in Caenorhabditis elegans. Genes Dev *23*, 496-511.

Speese, S., Petrie, M., Schuske, K., Ailion, M., Ann, K., Iwasaki, K., Jorgensen, E.M., and Martin, T.F. (2007). UNC-31 (CAPS) is required for dense-core vesicle but not synaptic vesicle exocytosis in Caenorhabditis elegans. J Neurosci *27*, 6150-6162.

Speidel, D., Varoqueaux, F., Enk, C., Nojiri, M., Grishanin, R.N., Martin, T.F., Hofmann, K., Brose, N., and Reim, K. (2003). A family of Ca2+-dependent activator proteins for secretion: comparative analysis of structure, expression, localization, and function. J Biol Chem *278*, 52802-52809.

Sternson, S.M., Nicholas Betley, J., and Cao, Z.F. (2013). Neural circuits and motivational processes for hunger. Curr Opin Neurobiol *23*, 353-360.

Stoeckman, A.K., Ma, L., and Towle, H.C. (2004). Mlx is the functional heteromeric partner of the carbohydrate response element-binding protein in glucose regulation of lipogenic enzyme genes. J Biol Chem *279*, 15662-15669.

Stoltzman, C.A., Peterson, C.W., Breen, K.T., Muoio, D.M., Billin, A.N., and Ayer, D.E. (2008). Glucose sensing by MondoA:Mlx complexes: a role for hexokinases and direct regulation of thioredoxin-interacting protein expression. Proc Natl Acad Sci U S A *105*, 6912-6917.

Taghert, P.H., and Nitabach, M.N. (2012). Peptide neuromodulation in invertebrate model systems. Neuron *76*, 82-97.

Trent, C., Tsuing, N., and Horvitz, H.R. (1983). Egg-laying defective mutants of the nematode Caenorhabditis elegans. Genetics *104*, 619-647.

Tschop, M., Smiley, D.L., and Heiman, M.L. (2000). Ghrelin induces adiposity in rodents. Nature *407*, 908-913.

Wark, B., Fairhall, A., and Rieke, F. (2009). Timescales of inference in visual adaptation. Neuron *61*, 750-761.

Wark, B., Lundstrom, B.N., and Fairhall, A. (2007). Sensory adaptation. Curr Opin Neurobiol *17*, 423-429.

Warren, C.E., Krizus, A., and Dennis, J.W. (2001). Complementary expression patterns of six nonessential Caenorhabditis elegans core 2/I N-acetylglucosaminyltransferase homologues. Glycobiology *11*, 979-988.

White, J.G., Southgate, E., Thomson, J.N., and Brenner, S. (1986). The structure of the nervous system of the nematode Caenorhabditis elegans. Philos Trans R Soc Lond B Biol Sci *314*, 1-340.

Figure Legends

Figure 1. Food deprivation specifically and reversibly alters repellent-driven behaviors. (A) Schematic of sensory integration assay with the copper barrier (blue) and animals at the origin and the attractant on the other side. (B) Food-deprived animals show increased integration index compared to well-fed animals integrating 50mM copper sulfate with 1:500 diacetyl. Two–tailed Student's *t* test ***$p < 0.0001$, $n \geq 9$. (C) Compared to well-fed animals, food-deprived animals

cross the copper sulfate barrier significantly more even when no attractant is presented in the assay. Chemotaxis to diacetyl alone is not modified by food deprivation. One sample *t* test ***p < 0.0001, n ≥ 9 per condition per assay. (D) Time course of food deprivation shows that a minimum two hours of food deprivation is required for modifying behavior. Maximum behavioral modification can be observed after three hours of food deprivation. One-way ANOVA ***p < 0.0001, n ≥ 9 per condition per time point. (E) After three hours of food deprivation, five hours of recovery on food reverts sensory integration behavior to well-fed levels. One-way ANOVA ***p < 0.0001, n ≥ 9 per condition per time point. (F) Animals exposed to aztreonam-treated *E. coli* for three hours show similar reduction in copper sensitivity as food-deprived animals. One sample *t* test p < 0.05, n ≥ 9 per condition. All bars represent population means; error bars indicate SEM. *See also Figure S1-S2, S7.*

Figure 2. Food deprivation reduces reorientation events enabling increased repellent barrier crossing. (A-B) Tracks of (A) well-fed and (B) food-deprived animals in sensory integration assay over 45 minutes. Blue line in the middle indicates the position of copper barrier. Animals begin -10 mm from copper barrier and diacetyl is positioned at 10mm from copper barrier at the orange spot. (n = 48 for each condition). (C) Reorientation probability of well-fed and food-deprived animals moving towards (left half) and away (right half) from the copper line during sensory integration assay. Well-fed animals exhibit increased reorientation probability approaching copper line. (D) Small-turn probability of well-fed and food-deprived animals moving towards (left half) and away (right half) from the copper line during sensory integration assay. Well-fed and food-deprived animals exhibit similar small-turn behaviors. All data points represent median of bootstrap reorientation probability estimates; error bars indicate 50% bootstrap bias-corrected confidence interval (n > 100, bootstraps = 1000, * 95% CI). *See also Figure S3.*

Figure 3. Multiple tissues sense lack of food with MML-1, process and release neuropeptides to modify behavior upon food deprivation. (A) *mml-1*, but not *mxl-2* mutants are defective in modifying integration responses after food deprivation. Restoring *mml-1* cDNA in the intestine or body wall muscles but not neurons is sufficient to restore normal food deprivation behavior to *mml-1* mutants. (B) Schematic representation of promoters used for

tissue-specific expression. Pan-neuronal expression is achieved using *unc-119 or H20* promoter, intestine expression using *gly-19* promoter, body wall muscle expression using *myo-3* promoter, pharyngeal muscle expression using *myo-2* promoter, and tail hypodermal cell expression using *lin-44* promoter. (C) Schematic representation of proteins required for neuropeptide processing and release. Pro-peptides are cleaved by pro-protein convertases (AEX-5, EGL-3, BLI-4 and KPC-1) and further processed before they are packed into dense core vesicles and released using UNC-31 (CAPS protein). (D) AEX-5 and EGL-3, but not BLI-4 or KPC-1 processed peptides are required for sensory integration change after food deprivation. (E) Tissue-specific rescues of *aex-5* in either intestine, body wall muscles or neurons reverts *aex-5* null mutants to normal sensory integration response after food deprivation. (F) Tissue-specific knockdown of *aex-5* in wild-type animals in intestine, body wall muscles or neurons resulted in animals that were defective in integration response after food deprivation. (G) Tissue-specific knockdown of *unc-31* in the intestine, body wall muscles or neurons of wild-type animals does not modify integration behavior after food deprivation, supporting a requirement for neuropeptide release from these tissues. All bars represent population means; error bars indicate SEM. Unpaired *t* test with Welch's correction *$p < 0.05$; **$p < 0.001$; ***$p < 0.0001$, $n \geq 9$ per condition per strain.

Figure 4. ASI chemosensory neurons use DAF-2 receptors to integrate intestine-released neuropeptides. (A) *daf-2* mutants are defective in their sensory integration response after food deprivation. Rescue of *daf-2* in neurons, but not intestine or body wall muscles, is sufficient to restore wild-type food deprivation behavior. (B) Restoring DAF-2 to ASI, but not ASH or ADL neurons, is sufficient to partially restore integration response after food deprivation to *daf-2* mutants. (C) Schematic diagram of candidate pathway components downstream of DAF-2 activation. Components in green are required for behavioral modification upon food deprivation. (D) Animals with mutations in the *sgk-1* and *rict-1* genes are defective in integration response to food deprivation. Restoring *sgk-1* and *rict-1* to ASI neurons is sufficient to restore food-deprivation induced behavioral modification in s*gk-1 and rict-1* mutants, respectively. (E) Rescue of *aex-5* in the intestine and *daf-2* in ASI neurons of *aex-5;daf-2* double mutants is sufficient to restore sensory integration response after food deprivation. Unpaired *t* test with Welch's correction *$p < 0.05$; **$p < 0.001$; ***$p < 0.0001$, $n \geq 9$ per condition per strain. *See also Figure S4.*

Figure 5. Food deprivation alters ASI neuronal adaptation rate. (A) Responses of ASI neurons to 1-second pulses of 50mM copper solution in wild-type well-fed (WF) and food-deprived (FD) animals. Gray bars (16) represent stimulus pulses. Food-deprived animals do not readily adapt to repeated repellent pulses. Solid lines represent averaged traces, shading around each line indicate SEM ($n \geq 21$). (B) Bar graph of averaged fluorescence over a 8s-window before and after peak response (red arrow in (A) indicates peak). Well-fed animals respond to copper with an increase leading to the peak response followed by decay after the peak. In contrast, ASI responses in food-deprived animals continue to rise to subsequent pulses. Error bar indicates SEM (Unpaired *t* test with Welch's correction, $*p < 0.05$, $**p < 0.001$, $n \geq 21$). (C) Responses of ASH neurons to 1-second pulses of 50mM copper solution in well-fed and food-deprived animals. Solid lines represent averaged traces, shading around each line indicate SEM ($n \geq 21$). (D) Bar graph of averaged fluorescence over a 8s-window before and after peak response (red arrow in (C) indicates peak). ASH neurons in well-fed and food-deprived animals respond similarly to copper before and after the peak. Error bar indicates SEM (Unpaired *t* test with Welch's correction, $*p < 0.05$, $n \geq 21$). *See also Figure S5 – S6.*

Figure 6. Modification of ASI neuronal adaptation rate after food deprivation requires DAF-2 signaling. (A) Responses of ASI neurons to 1-second pulses of 50 mM copper solution in *daf-2* mutant animals under well-fed (WF) and food-deprived (FD) conditions. Gray bars (16) represent stimulus pulses. WF and FD *daf-2* animals respond similarly to copper stimuli. Solid lines represent averaged traces, shading around each line indicate SEM ($n \geq 13$). (B) Bar graph of averaged fluorescence over a 8s-window before and after peak response (red arrow in (A) indicates peak). Well-fed and food-deprived *daf-2* mutants respond to copper with an increase leading to the peak response followed by decrease after the peak. Error bar indicates SEM (Unpaired *t* test with Welch's correction, $*p < 0.05$, $n \geq 13$). (C) Responses of ASH neurons to 1-second pulses of 50mM copper solution in well-fed and food-deprived *daf-2* animals. Solid lines represent averaged traces, shading around each line indicate SEM ($n \geq 13$). (D) Bar graph of averaged fluorescence over a 8s-window before and after peak response (red arrow in (C) indicates peak). ASH neurons in well-fed and food-deprived animals respond similarly to copper before and after the peak. Error bar indicates SEM (Unpaired *t* test with Welch's correction, *p <

905 0.05, n ≥ 13). (E) Percent increase of post-peak response compared to pre-peak response. Wild-
906 type food-deprived ASI, but not ASH neurons show a significant increase in their response to
907 copper stimuli even as the responses decline in well-fed condition. Moreover, these food
908 deprivation effects on ASI neurons are lost in *daf-2* mutants. (F) Model for food-deprivation
909 induced modification of copper sensitivity. *See also Figure S5 –S6.*
910
911
912

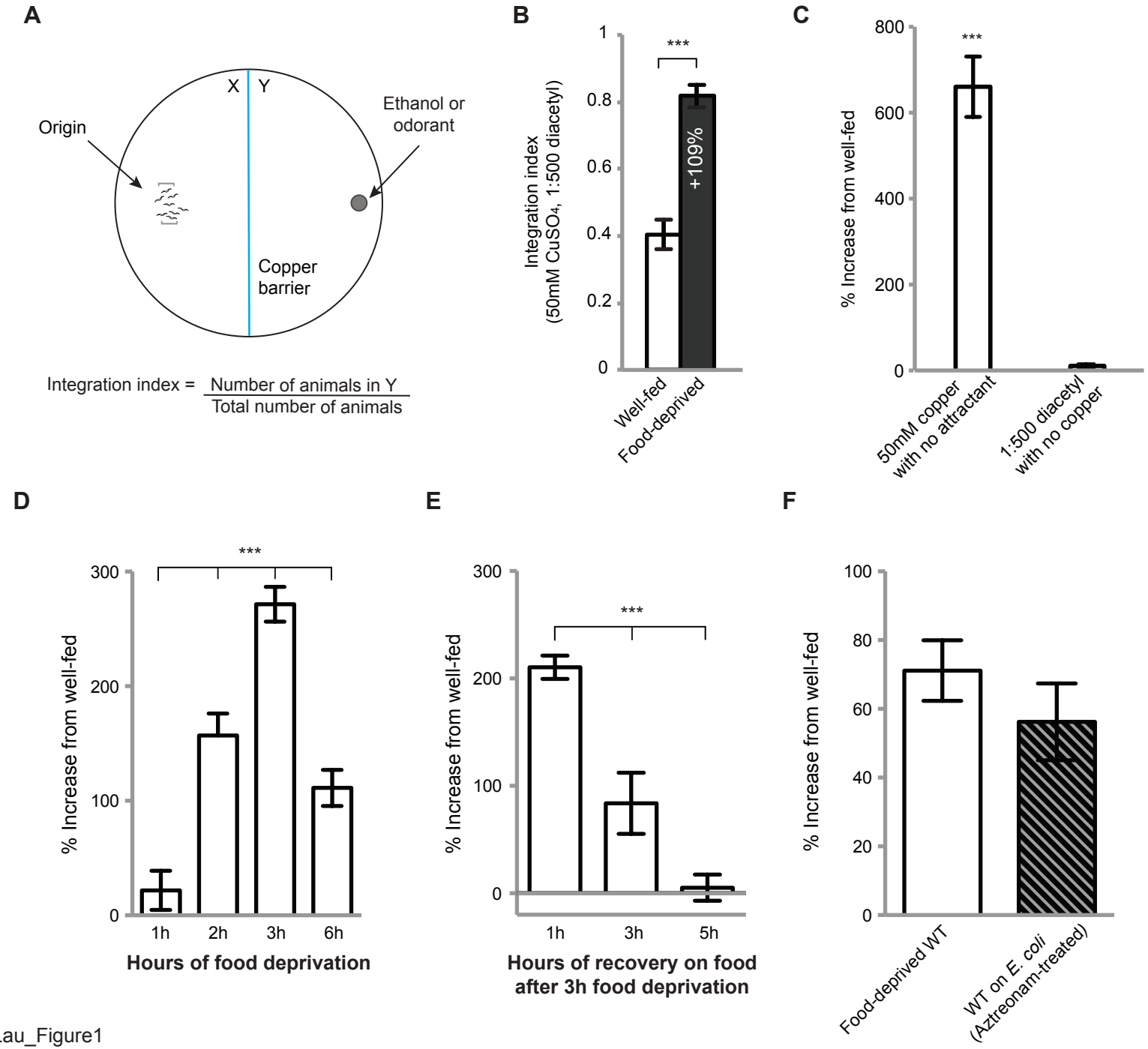
A
X
Y
Origin
Ethanol or odorant
Copper barrier
Integration index = Number of animals in Y / Total number of animals
B
Integration index (50mM CuSO4, 1:500 diacetyl)
***
+109%
Well-fed
Food-deprived
C
% Increase from well-fed
***
50mM copper with no attractant
1:500 diacetyl with no copper
D
% Increase from well-fed
***
1h
2h
3h
6h
Hours of food deprivation
E
% Increase from well-fed
***
1h
3h
5h
Hours of recovery on food after 3h food deprivation
F
% Increase from well-fed
Food-deprived WT
WT on E. coli (Aztreonam-treated)

Lau_Figure1

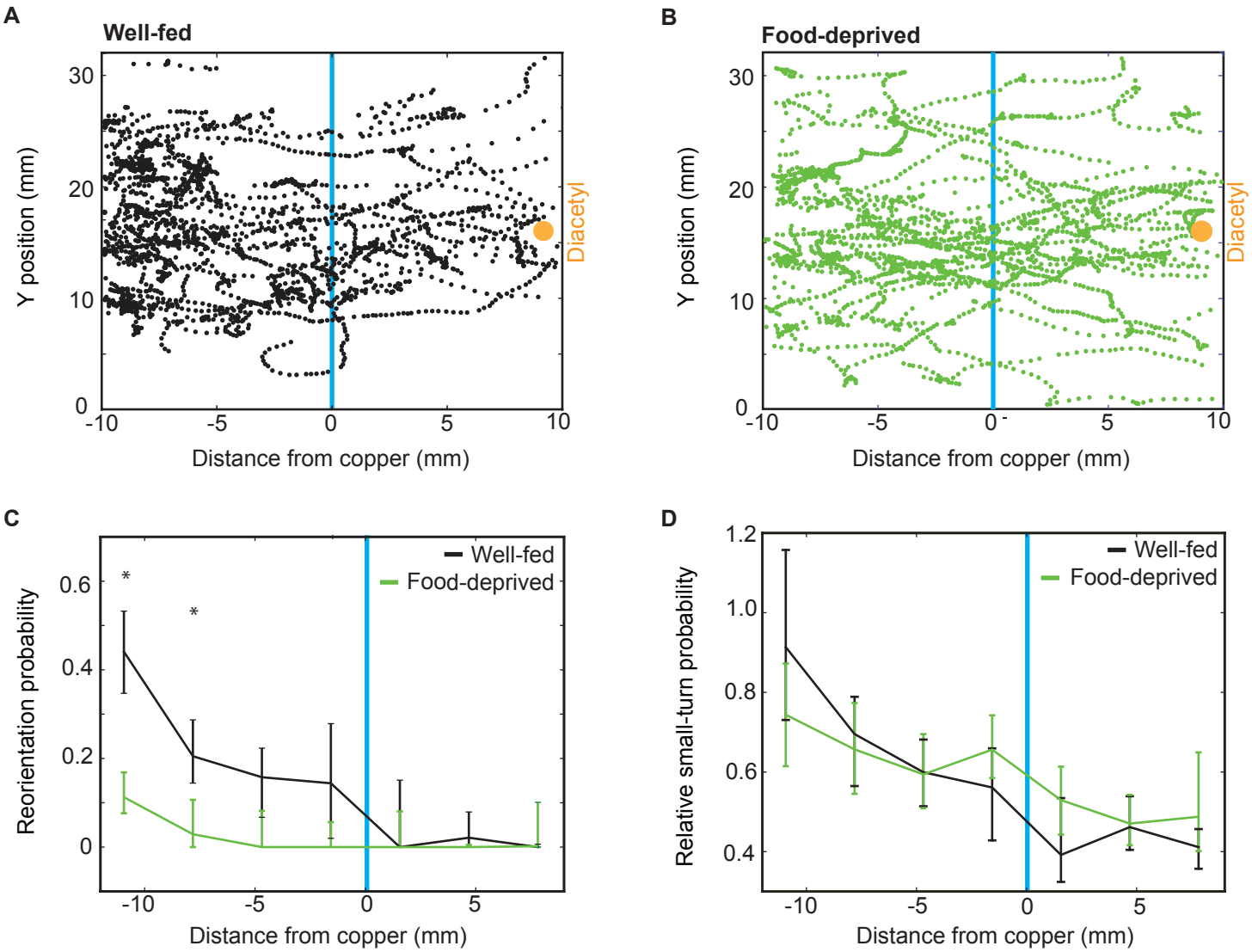

Lau_Figure2

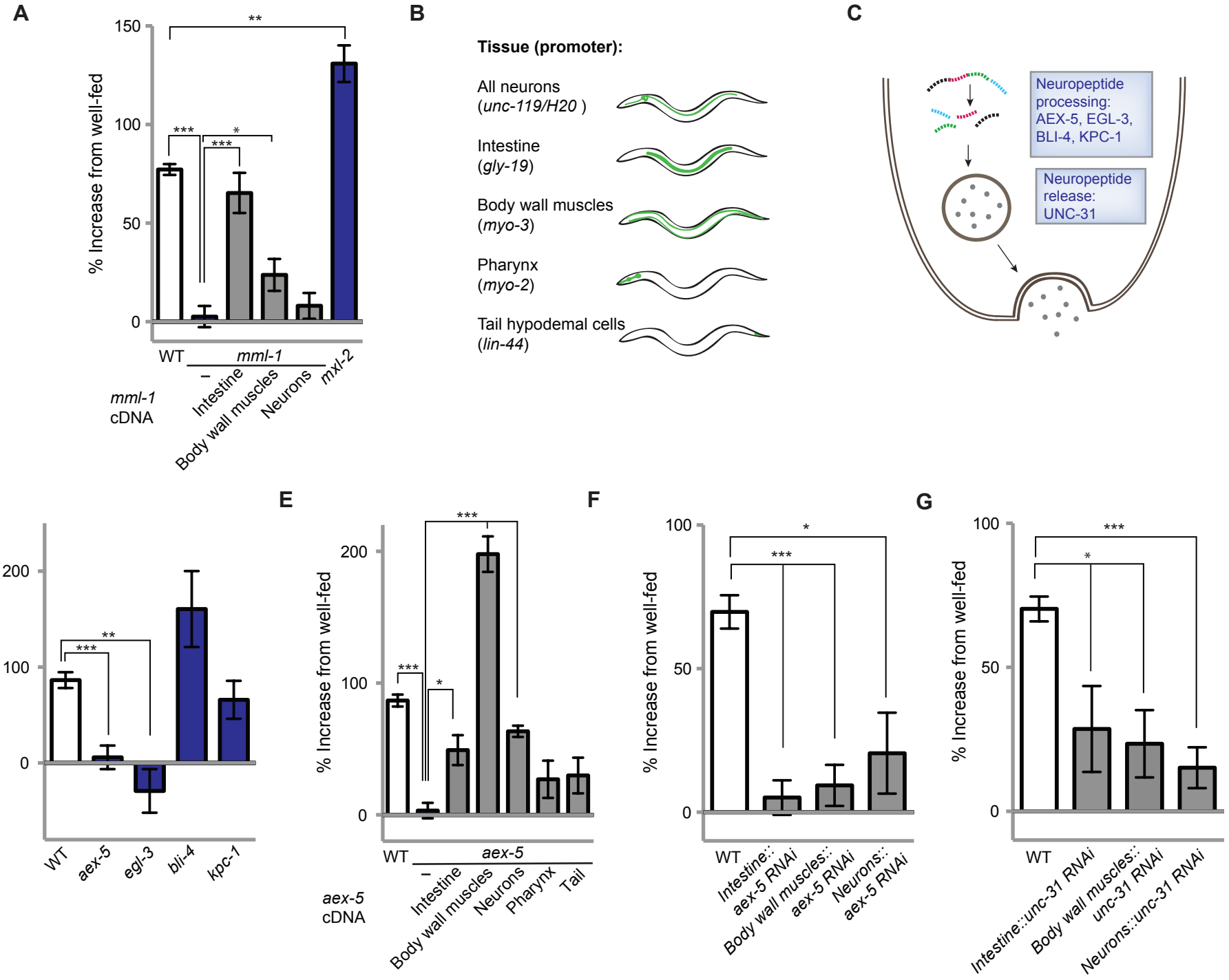
A
% Increase from well-fed
150
100
50
0
**
***
*
***
WT
mml-1
–
Intestine
Body wall muscles
Neurons
mxl-2
mml-1
cDNA
B
Tissue (promoter):
All neurons
(unc-119/H20)
Intestine
(gly-19)
Body wall muscles
(myo-3)
Pharynx
(myo-2)
Tail hypodemal cells
(lin-44)
C
Neuropeptide
processing:
AEX-5, EGL-3,
BLI-4, KPC-1
Neuropeptide
release:
UNC-31
D
% Increase from well-fed
200
100
0
**
***
WT
aex-5
egl-3
bli-4
kpc-1
E
% Increase from well-fed
200
100
0
***
***
*
WT
aex-5
–
Intestine
Body wall muscles
Neurons
Pharynx
Tail
aex-5
cDNA
F
% Increase from well-fed
100
50
0
*
***
WT
Intestine::
aex-5 RNAi
Body wall muscles::
aex-5 RNAi
Neurons::
aex-5 RNAi
G
% Increase from well-fed
100
50
0
***
*
WT
Intestine::unc-31 RNAi
Body wall muscles::
unc-31 RNAi
Neurons::unc-31 RNAi

Lau_Figure3

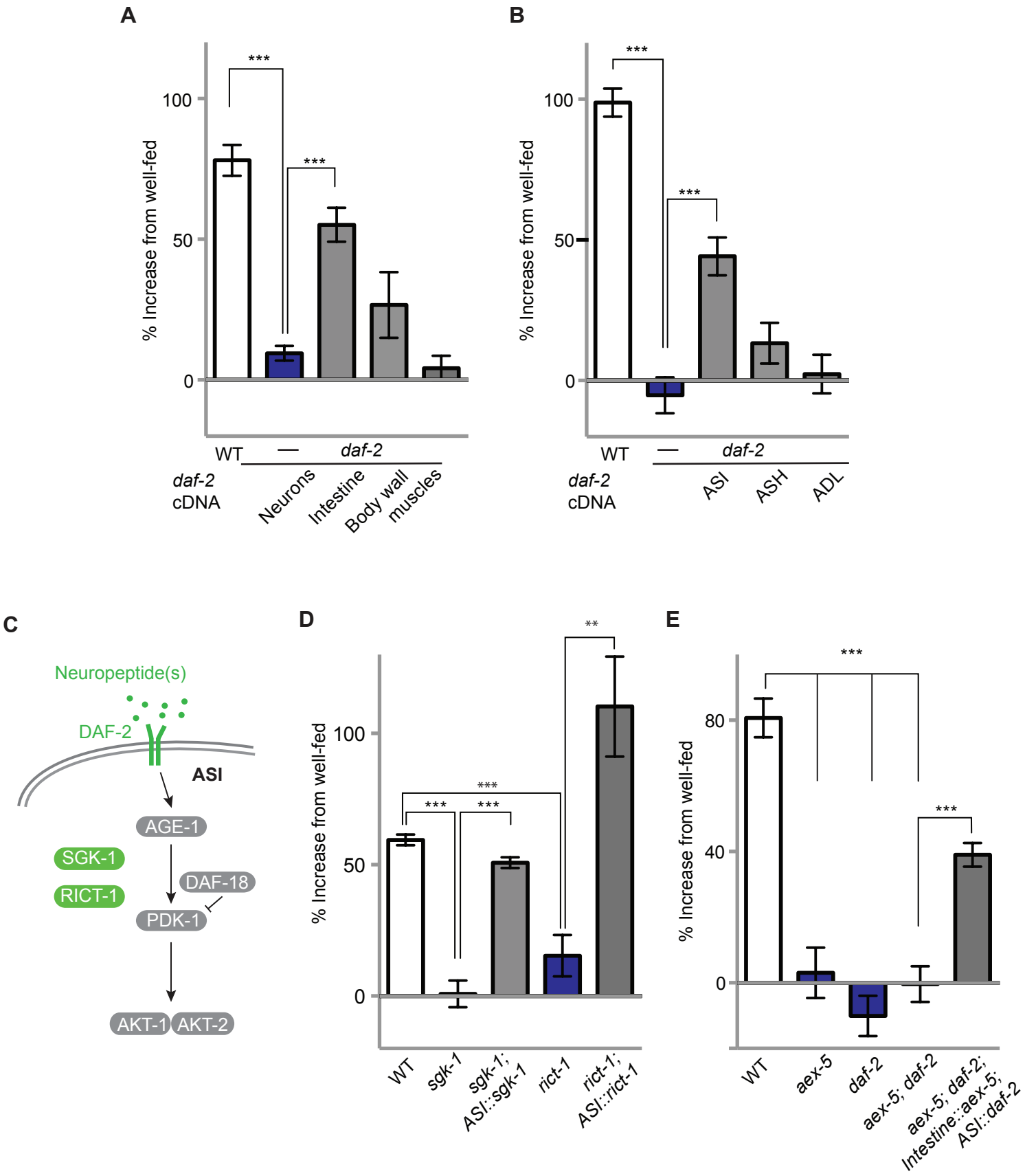

Lau_Figure4

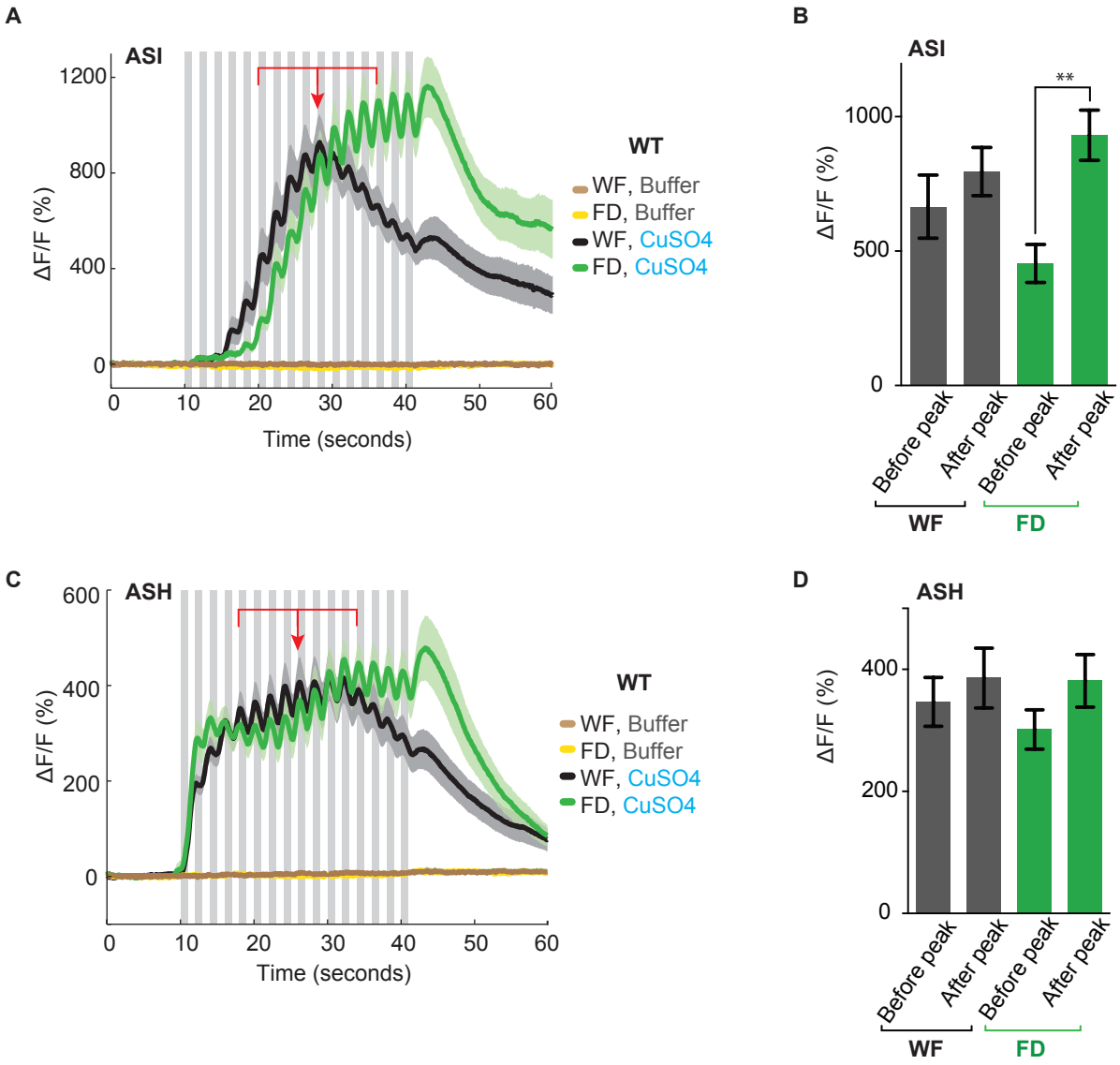

Lau_Figure5

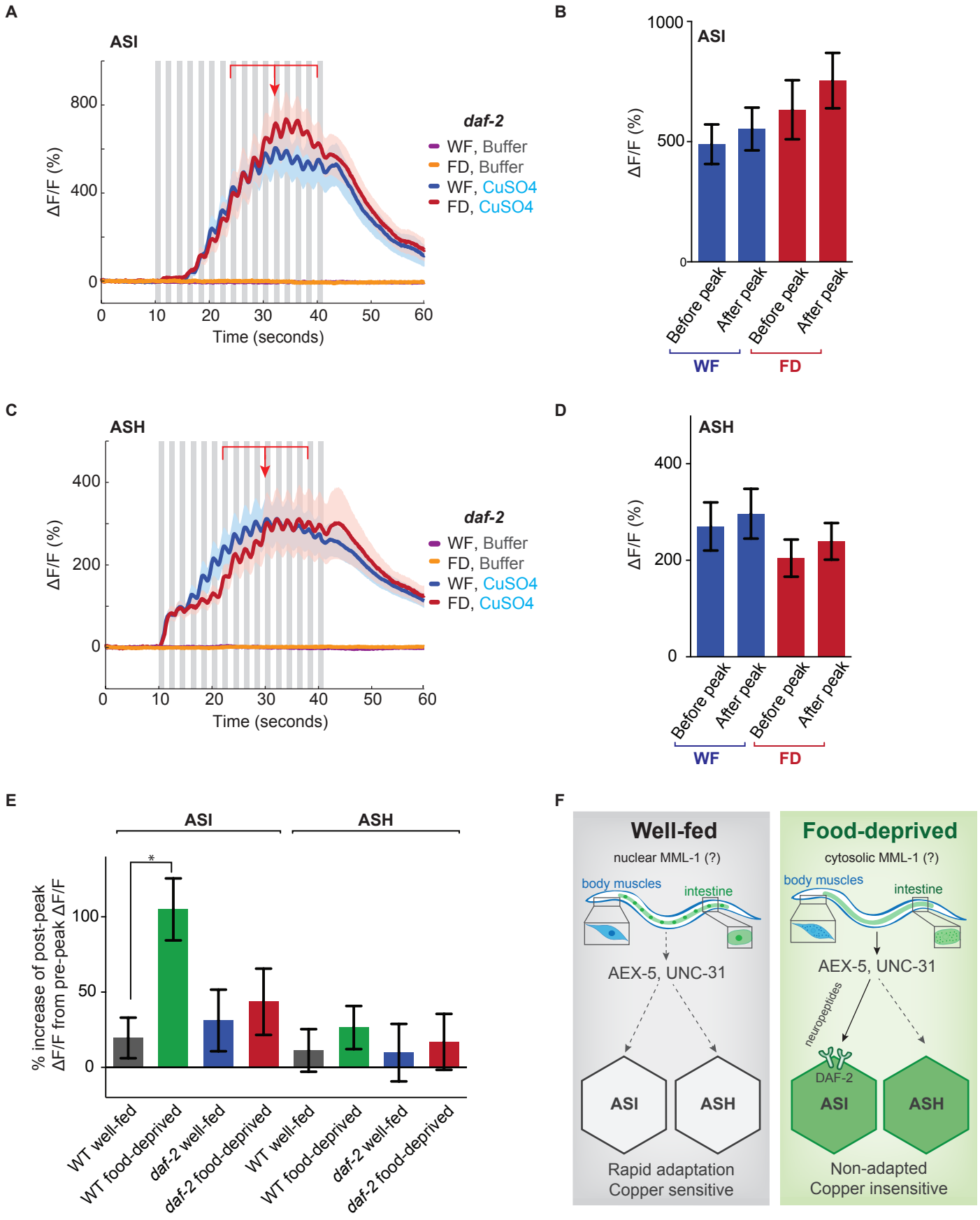

Lau_Figure6